Probing proton cross-shell excitations through the two-neutron removal from ^{38}Ca to ^{36}Ca

T. Beck,[1,*] A. Gade,[1,2] B.A. Brown,[1,2] J.A. Tostevin,[3] D. Weisshaar,[1] D. Bazin,[1,2] K.W. Brown,[1,4] R.J. Charity,[5] P.J. Farris,[1,2] S.A. Gillespie,[1] A.M. Hill,[1,2] J. Li,[1] B. Longfellow,[1,2,†] D. Rhodes,[1,2,‡] and W. Reviol[6]

[1] *Facility for Rare Isotope Beams, Michigan State University, East Lansing, Michigan 48824, USA*
[2] *Department of Physics and Astronomy, Michigan State University, East Lansing, Michigan 48824 USA*
[3] *Department of Physics, Faculty of Engineering and Physical Sciences, University of Surrey, Guildford, Surrey GU2 7XH, United Kingdom*
[4] *Department of Chemistry, Michigan State University, East Lansing, Michigan 48824 USA*
[5] *Department of Chemistry, Washington University, St. Louis, Missouri 63130 USA*
[6] *Physics Division, Argonne National Laboratory, Argonne, Illinois 60439 USA*

(Dated: September 15, 2023)

Bound states of the neutron-deficient, near-dripline nucleus ^{36}Ca were populated in two-neutron removal from the ground state of ^{38}Ca, a direct reaction sensitive to the single-particle configurations and couplings of the removed neutrons in the projectile wave function. Final-state exclusive cross sections for the formation of ^{36}Ca and the corresponding longitudinal momentum distributions, both determined through the combination of particle and γ-ray spectroscopy, are compared to predictions combining eikonal reaction theory and shell-model two-nucleon amplitudes from the USDB, USDC, and ZBM2 effective interactions. In this analysis, the final-state cross-section ratio $\sigma(2_1^+)/\sigma(0^+)$ shows particular sensitivity and is approximately reproduced only with the two-nucleon amplitudes from the ZBM2 effective interaction that includes proton cross-shell excitations into the pf shell. Characterizing the proton pf-shell occupancy locally and schematically, an increase of the *sd*-*pf* shell gap by 250 keV yields an improved description of this cross-section ratio and simultaneously enables a reproduction of the $B(E2;0_1^+ \rightarrow 2_1^+)$ excitation strength of ^{36}Ca. This highlights one of the important aspects if a new shell-model effective interaction for the region was to be developed on the quest to model the much discussed neutron-deficient Ca isotopes and surrounding nuclei whose structure is impacted by proton cross-shell excitations.

The calcium isotopic chain constitutes an attractive testing ground for nuclear models due to its diverse structure with changing neutron number, N. Besides the well-established magic numbers at $N = 20$ and 28, new neutron (sub-)shell closures have been identified for the neutron-rich ^{52}Ca [1–3] and ^{54}Ca [4, 5] isotopes at $N = 32$ and 34, respectively. At the neutron-deficient end of the calcium isotopic chain, a recent mass measurement of ^{35}Ca suggests a doubly-magic character also for ^{36}Ca ($N = 16$) [6]. Due to their location at the northern boundary of the *sd* shell, the nuclear structure of the calcium isotopes is highly susceptible to the occupation of proton pf-shell orbitals. However, calculations using nuclear density functional theory, which were employed for the description of nuclear charge radii, indicate only a small proton pf-shell occupancy in the ground state [7], thus largely leaving the $Z = 20$ shell closure intact. Studies of the nucleus ^{36}Ca using configuration-interaction shell-model calculations [8] corroborate these results [9, 10] but identify an almost pure proton $2p$-$2h$ intruder configuration for the first excited 0_2^+ state. This interesting level exhibits one of the largest known mirror-energy differences on the nuclear chart [9], which was subsequently confirmed experimentally through a combination of (p,d) and (p,t) transfer reactions [10].

In contrast to the findings above, an earlier shell-model study of nuclear charge radii was interpreted to indicate a considerable weakening of the $Z = 20$ and $N = 20$ shell closures already in the vicinity of doubly magic ^{40}Ca [11]. Due to the possibility of proton excitations, a weakened $Z = 20$ shell closure should also result in enhanced quadrupole collectivity of the neutron-deficient calcium isotopes. Indeed, the successful description of the measured $B(E2;0_1^+ \rightarrow 2_1^+)$ transition strengths of ^{36,38}Ca was shown to require the incorporation of sizable proton pf-shell occupancy in the ground states [12]. In contrast, the USDB Hamiltonian, which is limited to the *sd* model space [13], underestimates the excitation strength by about one order of magnitude, presumably due to the absence of proton excitations. Enlarging the model space to include the pf shell and employing the SDPF-U-MIX effective interaction [14], which yields a good description of the low-energy structure and mirror-energy differences of the ^{36}Ca-^{36}S pair [9, 10], offers only a small increase relative to the USDB results and fails to adequately account for the low-lying collectivity of ^{36,38}Ca [12]. This quadrupole collectivity seems solely captured by the ZBM2 effective interaction in the $(1d_{3/2}, 2s_{1/2}, 1f_{7/2}, 2p_{3/2})$ model space [11], which predicts proton *sd* shell occupancies of merely 55 and 40% in the ground states of ^{36}Ca and ^{38}Ca, respectively [12]. In the future, the emerging evidence for the influence of

* beck@frib.msu.edu
† Present address: Lawrence Livermore National Laboratory, Livermore, California 94550, USA
‡ Present address: TRIUMF, 4004 Wesbrook Mall, Vancouver, BC V6T 2A3, Canada

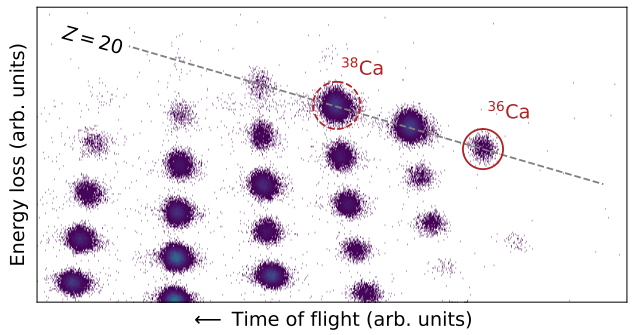

FIG. 1. Event-by-event particle identification plot of projectile-like residues produced in the ^{9}Be(^{38}Ca,$X+\gamma$)Y reaction. The figure displays the data used for determination of absolute inclusive cross sections and has a particle-γ coincidence condition applied. Inelastically scattered ^{38}Ca beam entering the focal plane and the ^{36}Ca two-neutron removal residues are marked.

proton cross-shell excitations could be tested and quantified through direct proton-removal reactions.

Here, the direct two-neutron removal reaction from ^{38}Ca is used to gain valuable and complementary insights into the wave-function overlap of the ground state of ^{38}Ca and the bound final states of ^{36}Ca. The associated final-state exclusive cross sections are modeled through a combination of eikonal reaction dynamics and shell-model two-nucleon amplitudes (TNAs) [15, 16]. The latter, which encode the overlap between the initial and final states, facilitate a sensitive and unique benchmark of different model spaces and interactions when confronting the measured and theoretical cross sections. In the present case of two-neutron removal from the ground state of ^{38}Ca to bound final states of ^{36}Ca, calculated cross sections $\sigma^{\rm th}$, employing the USDB, USDC, and ZBM2 interactions, are compared to experimental values from the ^{9}Be(^{38}Ca,^{36}Ca+γ)X reaction to explore the adequacy of the pure *sd* shell (USDB and USDC) and the need for proton cross-shell excitations across the $Z = 20$ shell gap (ZBM2).

The unstable secondary ^{38}Ca beam was produced through fragmentation of a stable ^{40}Ca beam, accelerated by the Coupled Cyclotron Facility of the National Superconducting Cyclotron Laboratory [17] to 140 MeV/u, impinging on a 799-mg/cm^2 ^{9}Be production target and separated using a 300 mg/cm^2 Al wedge degrader in the A1900 fragment separator [18]. The momentum acceptance of the separator was limited to $\Delta p/p = 0.25$ %. The resulting secondary beam, which exhibited an approximately 85% purity in ^{38}Ca and a typical rate of $1.6 \cdot 10^5$ ^{38}Ca ions per second, was impinged on a secondary 188 mg/cm^2 thick ^{9}Be target located at the target position of the S800 magnetic spectrograph [19]. The midtarget energy of the ^{38}Ca projectiles was 60.9 MeV/u, corresponding to a velocity of $v/c \approx 0.345$.

The particle identification in the entrance and exit channel was performed on an event-by-event basis using plastic timing scintillators and the S800 focal-plane detection system [20]. The incoming projectiles were identified from their velocity difference measured between two plastic scintillators located at the exit of the A1900 and the object position of the S800 analysis beam line. The outgoing reaction residues were distinguished based on their energy loss determined in the S800 ionization chamber and the time of flight measured between the object position of the analysis beam line and the plastic scintillator at the back of the S800 focal plane. As evident from the particle-identification plot shown in Fig. 1, the ^{36}Ca nuclei produced in two-neutron removal are well separated from the other reaction residues entering the large-acceptance focal plane of the S800 spectrograph. Results from additional reaction channels populated in this experiment are reported in Refs. [21–23].

For detection of γ rays emitted in the decay of excited nuclear states, the reaction target was surrounded by the high-resolution γ-ray tracking array GRETINA [24, 25], consisting of twelve detector modules; each of which contains four 36-fold segmented high-purity germanium crystals. The Doppler-corrected γ-ray spectrum of ^{36}Ca produced in two-neutron removal from ^{38}Ca is shown in Fig. 2. The event-by-event Doppler reconstruction was performed with respect to the spatial coordinates of the γ-ray interaction point with the highest energy deposition as deduced from online signal decomposition. The spectrum features a prominent peak at 3046(3) keV, corresponding to the transition of the 2_1^+ state to the ground state. Testament to the proximity of the proton dripline, the low proton-decay threshold of ^{36}Ca of $S_p = 2570(40)$ keV [26] leaves the 2_1^+ state with a small proton decay branch in addition to the γ emission. In agreement with previous γ-ray spectroscopy [12, 27, 28], no transitions from the other excited states reported in Ref. [10] are observed. The recently discovered 0_2^+ state at 2.83(13) MeV is not only the first excited state of ^{36}Ca [10] but is also located above S_p. Depending on the Q value, it may decay via proton emission to the $3/2^+$ ground state of ^{35}K or de-excite via an isomeric [9] $E0$ transition to the ^{36}Ca ground state. At present, the Q-value uncertainty exceeds 50% and a dominance of either decay branch is possible.

The S800 magnetic rigidity was optimized on ^{36}Ca, allowing for ions with momenta of approximately ± 0.300 GeV/c around central momentum $p_0 = 11.222$ GeV/c to enter the spectrometer's focal plane. Fig. 3(a) shows the measured inclusive parallel momentum distribution of ^{36}Ca produced in two-neutron removal from ^{38}Ca. Employing a software gate on the observed $2_1^+ \rightarrow 0_1^+$ transition in the γ-ray spectrum (Fig. 2), the partial $p_{\parallel}$ distribution for the ^{36}Ca left in the 2_1^+ final state was extracted. The parallel momentum distribution obtained after subtraction of the 2_1^+ from the inclusive $p_{\parallel}$ distribution now comprises contributions from the 0_1^+ ground state and also any contribution from the 0_2^+ excited state if it is proton bound as the resulting isomeric $E0$ decay [9] will escape detection. These final-state ex-

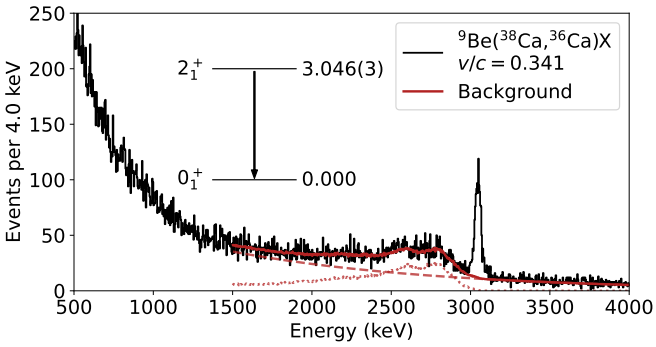

FIG. 2. Doppler-corrected ($v/c = 0.341$) γ-ray spectrum detected by GRETINA in coincidence with ^{36}Ca residues registered in the focal plane of the S800 spectrograph. The solid red curve represents a background model comprising an exponential component (dashed red) and GRETINA's detector response (dotted red) obtained from simulations employing the Geant4-based [29, 30] code UCGretina [31].

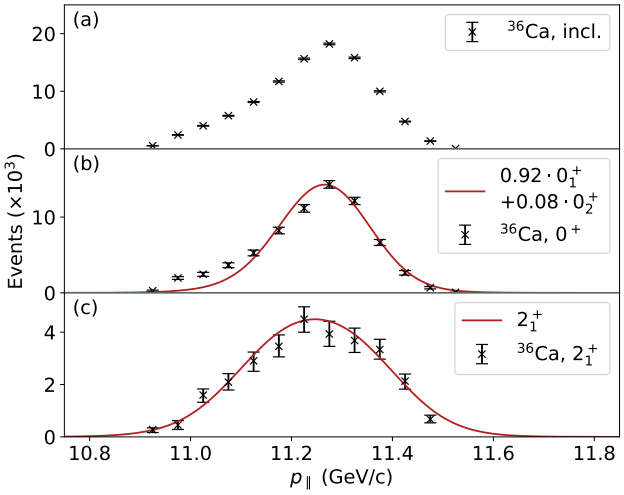

FIG. 3. Parallel momentum distributions of ^{36}Ca after two-neutron removal from ^{38}Ca. (a) shows the inclusive $p_\parallel$ distribution which is fully within the S800 acceptance. The uncertainties are purely statistical. (b) and (c) display the exclusive $p_\parallel$ distributions to the 0^+ and 2_1^+ states, respectively. They are compared to calculations using ZBM2 TNAs (red lines) which are horizontally shifted and vertically scaled for best agreement with the data. The calculation for (b) is the sum of the 0_1^+ and 0_2^+ contributions according to their predicted cross sections (Table I). Due to the unknown proton decay branch, the 0_2^+ contribution is an upper limit.

clusive parallel momentum distribution are displayed in Fig. 3(b) and (c).

Theoretical calculations of $p_\parallel$ distributions were obtained from eikonal reaction theory with the ZBM2 shell-model two-nucleon amplitudes as the nuclear-structure input. Since two-neutron removal from a neutron-deficient nucleus, as here, proceeds as a direct reaction [15, 16, 32, 33], the widths and shapes of the parallel momentum distributions have sensitivity to the total angular momentum of the removed nucleons [34, 35] and also to the orbital angular momentum couplings of the two nucleons [36]. Recently, the spectroscopic capabilities of $p_\parallel$ analyses were demonstrated for neutron-deficient *sd*-shell nuclei [37]. In order to facilitate a comparison to experimental $p_\parallel$ distributions, the symmetric theoretical distributions are transformed to the laboratory frame and folded with a rectangular function modeling the momentum difference due to the spatial extent of the target in the beam direction. The resulting distributions are furthermore convoluted with experimental $p_\parallel$ distributions of inelastically scattered beam particles in coincidence with γ rays above 1000 keV. This last step introduces a slight asymmetry and facilitates an empirical description of the low-momentum tails frequently encountered in intermediate-energy nucleon-removal reactions [37, 38]. As demonstrated in Fig. 3(b) and (c), the shapes of the calculated distributions obtained from this procedure agree well with the experimental ones and display the characteristic difference in widths for the different total angular momenta, J^π, while the low-momentum tail in the 0^+ distribution remains slightly underestimated.

We note that since the two-neutron removal occurs from the $J = 0$ ground state of ^{38}Ca, the total angular momentum of the removed neutrons uniquely determines the total angular momentum of the populated final state of ^{36}Ca, confirming the previous J^π assignments [12, 27, 28]. For the present case, the parallel momentum distributions calculated with the TNAs from the various shell-model effective interactions are essentially indistinguishable and cannot discriminate between the nuclear-structure input, unlike the cross sections discussed in the following.

The inclusive two-neutron removal cross section for the formation of ^{36}Ca was determined from the efficiency-corrected number of ^{36}Ca residues detected in the S800 focal plane, the number of incident ^{38}Ca projectiles, and the areal density of the target. It amounts to $\sigma_{\rm inc} = 0.408(9)_{\rm stat}(12)_{\rm syst}$ mb and is corrected for the known, small proton decay branch of the 2_1^+ state [12]. Employing particle-γ coincidences, the exclusive cross sections to the 0^+ and 2_1^+ states are obtained; the former more than twice as large as the latter (see Table I). Due to the low proton-separation threshold, the existence of sizable unobserved feeding can be excluded. Lacking a γ-ray detectable in GRETINA, exclusive cross sections to the 0_1^+ and 0_2^+ states are indistinguishable. In the following, their summed cross section is denoted $\sigma(0^+) = \sigma(0_1^+) + \sigma(0_2^+)$. In Table I, the measured cross sections are compared to calculations from eikonal reaction theory incorporating shell-model TNAs from the USDB [13], USDC [39], and ZBM2 [11] interactions. Due to the uncertain proton decay branch, the calculated two-neutron removal cross sections to the 0_2^+ state are an upper limit.

TABLE I. Comparison of experimental and calculated two-neutron removal cross sections from ^{38}Ca to final states of ^{36}Ca on a ^{9}Be target. Since only the sum of cross sections to the 0^+_1 and 0^+_2 states, $\sigma(0^+) = \sigma(0^+_1) + \sigma(0^+_2)$, is experimentally accessible, the theoretical cross sections are treated accordingly. In the case of the USDB and USDC shell-model effective interactions, the reported 0^+_2 intruder state is outside the model space.

		Experiment	ZBM2 [11]	ZBM2gap	USDB [13]	USDC [39]
σ (mb)	0^+_1	$0.292(8)_{\rm stat}(8)_{\rm syst}$ [1]	0.654	0.637	0.609	0.625
	0^+_2		0.058	0.064		
	2^+_1	$0.116(6)_{\rm stat}(3)_{\rm syst}$	0.140	0.192	0.824	0.824
	inclusive	$0.408(9)_{\rm stat}(12)_{\rm syst}$	0.851	0.893	1.433	1.449
R_s(2N)			$0.479(10)_{\rm stat}(14)_{\rm syst}$	$0.457(10)_{\rm stat}(13)_{\rm syst}$	$0.285(6)_{\rm stat}(8)_{\rm syst}$	$0.282(6)_{\rm stat}(8)_{\rm syst}$
$\sigma(2^+_1)/\sigma(0^+)$		0.396(26)	0.197	0.274	1.353	1.318

[1] Combined cross section to the 0^+_1 and 0^+_2 states.

Differences in the absolute values of the measured and calculated inclusive cross sections are typically discussed in terms of the ratio $R_s(2\mathrm{N}) = \sigma^{\rm expt}_{\rm inc}/\sigma^{\rm th}_{\rm inc}$ [16]. Accounting for the inseparability of $\sigma^{\rm expt}(0^+_1)$ and $\sigma^{\rm expt}(0^+_2)$ if the 0^+_2 level is proton bound, cross sections to both states are included in the ZBM2 value of $\sigma^{\rm th}_{\rm inc}$ along with the 2^+_1 state whose population is revealed through the γ-ray spectrum (Fig. 2) and known proton branch [12]. For the *sd*-shell restricted USDB and USDC calculations the 0^+ intruder state is outside the model space. In fact, the first excited 0^+ state calculated with the USD interactions is similar in nature to the 0^+_3 level of ZBM2, almost 2 MeV above S_p, and would predominantly decay via proton emission. The body of available two-neutron removal data from *sd*-shell nuclei suggests values of around 0.5 for R_s(2N) [16, 33, 37]. As evident from Fig. 4(a), this is the case for the calculations using the ZBM2 TNAs. Those using the TNAs from the USD family of effective interactions, on the other hand, yield appreciably smaller R_s(2N) values.

Additional guidance is obtained from the ratios of the final-state exclusive cross sections; in the present case of low proton-emission thresholds, only the cross-section ratio $\sigma(2^+_1)/\sigma(0^+)$ with an experimental value 0.396(26) is accessible. As shown in Fig. 4(b), the USD-type calculations limited to the *sd* shell fail to describe the cross-section ratio. The USDB (USDC) TNAs overpredict the cross-section ratio by a factor of 3.4 (3.3) (see Table I and Fig. 4). In the ZBM2 calculation, the *sd*-shell cross section is shared between the first and second 2^+ states, the latter proton unbound, yielding the near reproduction of the observed $\sigma(2^+_1)/\sigma(0^+)$ ratio.

Figure 4 immediately indicates that only the cross-section calculations with the ZBM2 TNAs get close to the data, but are not yet in agreement. To explore the role of proton pf-shell occupation, schematically, we modify the *sd*-*pf* shell gap in ZBM2. With the gap increased by 250 keV, labeled as ZBM2gap, the fraction of proton closed-shell configuration in the ground state is raised from 55 to 62%. With ZBM2gap the cross-section ratio $\sigma(2^+_1)/\sigma(0^+)$ of Fig. 4(b) increases from 0.20 to 0.27, reducing the deviation from experiment and hinting that potentially fewer proton cross-shell excitations than present in ZBM2 are needed to match the measurement.

While this is not an attempt to propose a modification of ZBM2, but rather the exploration of the role of proton excitations, it is instructive to study the effect on the quadrupole collectivity as well, which is expected to be very sensitive to pf-shell proton occupancy. Employing the ZBM2gap interaction with the same effective charges as used in Ref. [12], $e_p = 1.36$ and $e_n = 0.45$, a $B(E2; 0^+_1 \to 2^+_1)$ value of $133\,e^2\mathrm{fm}^4$ for ^{36}Ca is obtained. This value is in better agreement with the measured transition strength of $B(E2; 0^+_1 \to 2^+_1) = 131(20)\,e^2\mathrm{fm}^4$ than the calculated value of $179\,e^2\mathrm{fm}^4$ obtained with the standard ZBM2 interaction [12]. This observation is also con-

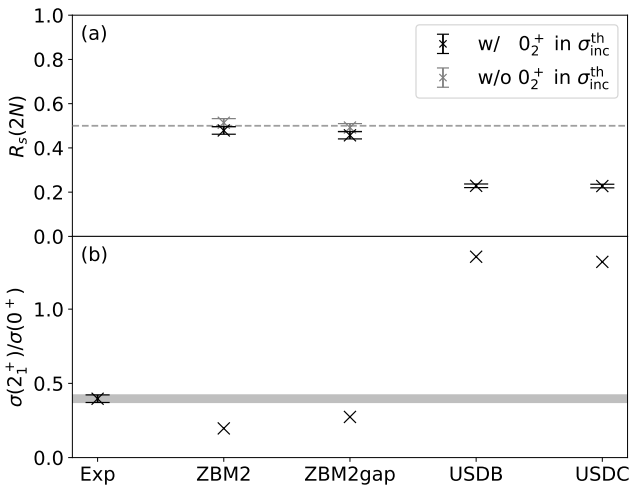

FIG. 4. Comparison of calculated and measured cross sections. (a) Measured to theoretical inclusive cross-section ratios $R_s(2\mathrm{N}) = \sigma^{\rm expt}_{\rm inc}/\sigma^{\rm th}_{\rm inc}$ [16] with (without) inclusion of the 0^+_2 state in the calculation of the theoretical inclusive cross section are shown in black (grey), illustrating the smallness of the 0^+_2 contribution. The expected value of 0.5 [16, 33, 37] is indicated by the grey dashed line. (b) Ratio of the exclusive cross sections to the 2^+_1 and 0^+ final states of ^{36}Ca. The 1σ region around the experimental result is indicated in gray. For this comparison, the statistical and systematic uncertainties are added in quadrature.

sistent with the suggestion above that likely less proton cross-shell excitations are needed to describe the structure of ^{36}Ca. However, the significant limitations of such a local, ad-hoc modification become apparent when comparing the measured and calculated $B(E2)$ values for ^{38}Ca. The $B(E2; 0_1^+ \rightarrow 2_1^+) = 68\, e^2\mathrm{fm}^4$ value calculated for ZBM2gap underestimates the measured value within three sigma [12] although being in better agreement than the *sd*-shell limited calculations.

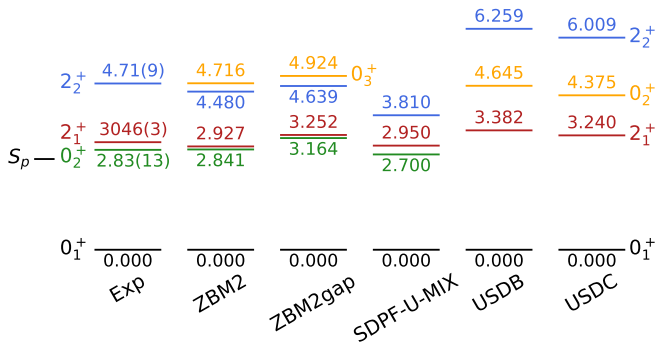

FIG. 5. Comparison of the partial experimental level scheme of ^{36}Ca with shell-model calculations. The measured 0_2^+ intruder state [10] is absent from the USD-type shell-model calculations and the second excited 0^+ state in the USD computations is closer in structure to the 0_3^+ state of ZBM2 and ZBM2gap. The experimental excitation energies of the 0_2^+ and 2_2^+ states as well as predictions from the SDPF-U-MIX interaction are taken from Ref. [10].

Lastly, excitation energies of low-lying states can yield further insight into the need for proton pf-shell occupation. As shown in Fig. 5, the USDB and USDC calculations do not reproduce the measured level ordering. Only the interactions incorporating proton cross-shell excitations into the pf shell, namely ZBM2, ZBM2gap, and SDPF-U-MIX, correctly place the 0_2^+ as the first excited state. In ZBM2, the 0_2^+ level is characterized by a 42% $2p$-$2h$ proton intruder component in the wave function; a weakening compared to the almost pure (82% $2p$-$2h$) intruder structure reported in Ref. [10]. A distinct difference, though, is found in the predicted energies for the 2_2^+ state at 4.71(9) MeV [10]. While calculations using the SDPF-U-MIX interaction, which identify it as an intruder state (79% $2p$-$2h$) similar to the 0_2^+ level, underestimate its excitation energy by approximately 0.90 MeV, the ZBM2 and ZBM2gap interactions enable a reproduction within 0.23 and 0.07 MeV, respectively.

Combining the conclusions drawn above, a clear picture emerges for ^{36}Ca. Solely the ZBM2 calculations are capable of describing the low-lying level schemes, reproducing the low-lying quadrupole collectivity, and capturing the division of the final-state exclusive two-neutron removal cross sections. Furthermore, ZBM2 (ZBM2gap) provide spectroscopic factors of 0.82 (0.86) and 0.42 (0.51) for the one-neutron transfer from ^{37}Ca to the 0_1^+ and 2_1^+ states of ^{36}Ca, respectively. It is evident that these are in better agreement with the experimental C^2S values of 1.06(22) and 0.66(14) than 0.94 (0.91) and 1.16 (1.01) obtained from the USDB (SDPF-U-MIX) interactions [10]. All of this is a clear affirmation of the importance of sizeable proton pf-shell components in the wave functions of the neutron-deficient ^{36,38}Ca nuclei as proposed in Refs. [11, 12]. For ^{36}Ca, in particular the ZBM2gap interaction that slightly modifies the pf-shell content allows for an improved description of the experimental $B(E2; 0_1^+ \rightarrow 2_1^+)$ and $\sigma(2_1^+)/\sigma(0^+)$ values. In this context, we note a mistake in the caption of Tab. VI of Ref. [12]. The reported results are erroneously attributed to standard ZBM2 interaction but were actually obtained from ZBM2gap [40].

In summary, the ^{9}Be(^{38}Ca,^{36}Ca+γ)X direct two-neutron removal reaction was used to populate bound states of ^{36}Ca. Final-state exclusive cross sections for the formation of ^{36}Ca in the 2_1^+ and ground state were deduced from particle-γ coincidence spectroscopy. Eikonal reaction dynamics employing as nuclear-structure input two-nucleon amplitudes from the shell-model effective interactions USDB, USDC, and ZBM2 help clarify the importance of proton pf-shell occupancy: The *sd*-shell restricted interactions USDB and USDC, which describe neither the low-energy spectrum nor the low-lying quadrupole collectivity of ^{36}Ca correctly, are also not able to reproduce the ratio of the cross sections to the two individual final states in the two-neutron removal reported here. The ZBM2 effective interaction in the $(1d_{3/2}, 2s_{1/2}, 1f_{7/2}, 2p_{3/2})$ model space, on the other hand, models the structure of the neutron-deficient calcium isotopes the best. With ZBM2 TNAs as input to the reaction model, a typical value of the measured to theoretical inclusive cross-section ratio R_s(2N) is obtained for the two-neutron removal from ^{38}Ca to ^{36}Ca and the ratio of the 0^+ and 2_1^+ exclusive cross sections is reproduced qualitatively. This agreement can be further improved by increasing the *sd*-*pf* shell gap in ZBM2 by 250 keV; this also brings the $B(E2; 0_1^+ \rightarrow 2_1^+)$ excitation strength of ^{36}Ca closer to the experimental result. Our new studies clearly demonstrate the need for proton cross-shell excitation into the pf shell already for the 0_1^+ and 2_1^+ states of ^{36}Ca, adding to the recent body of new data near the *sd*-shell model-space boundary. Ultimately, spectroscopic factors obtained from a proton removal reaction leading from ^{36}Ca to (unbound) pf-shell final states of the very weakly-bound dripline nucleus ^{35}K would surely quantify the pf-shell occupancy in the ground state of ^{36}Ca [12].

ACKNOWLEDGMENTS

This work was supported by the U.S. NSF under Grants No. PHY-1565546 and No. PHY-2110365, by the DOE NNSA through the NSSC, under Award No. DE-NA0003180, and by the U.S. DOE, Office of Science, Office of Nuclear Physics, under Grants No. DE-SC0020451 & DE-SC0023633 (MSU) and No. DE-FG02-87ER-40316

(WashU) and under Contract No. DE-AC02-06CH11357 (ANL). GRETINA was funded by the DOE, Office of Science. Operation of the array at NSCL was supported by the DOE under Grant No. DE- SC0019034. J. A. T. acknowledges support from the Science and Technology Facilities Council (U.K.) Grant No. ST/V001108/1.

[1] A. Huck, G. Klotz, A. Knipper, C. Miehé, C. Richard-Serre, G. Walter, A. Poves, H. L. Ravn, and G. Marguier, Beta decay of the new isotopes ^{52}K, ^{52}Ca, and ^{52}Sc; a test of the shell model far from stability, Phys. Rev. C **31**, 2226 (1985).

[2] F. Wienholtz, D. Beck, K. Blaum, C. Borgmann, M. Breitenfeldt, R. B. Cakirli, S. George, F. Herfurth, J. D. Holt, M. Kowalska, S. Kreim, D. Lunney, V. Manea, J. Menéndez, D. Neidherr, M. Rosenbusch, L. Schweikhard, A. Schwenk, J. Simonis, J. Stanja, R. N. Wolf, and K. Zuber, Masses of exotic calcium isotopes pin down nuclear forces, Nature **498**, 346 (2013).

[3] M. Rosenbusch, P. Ascher, D. Atanasov, C. Barbieri, D. Beck, K. Blaum, C. Borgmann, M. Breitenfeldt, R. B. Cakirli, A. Cipollone, S. George, F. Herfurth, M. Kowalska, S. Kreim, D. Lunney, V. Manea, P. Navrátil, D. Neidherr, L. Schweikhard, V. Somà, J. Stanja, F. Wienholtz, R. N. Wolf, and K. Zuber, Probing the $N = 32$ Shell Closure below the Magic Proton Number $Z = 20$: Mass Measurements of the Exotic Isotopes ^{52,53}K, Phys. Rev. Lett. **114**, 202501 (2015).

[4] D. Steppenbeck, S. Takeuchi, N. Aoi, P. Doornenbal, M. Matsushita, H. Wang, H. Baba, N. Fukuda, S. Go, M. Honma, J. Lee, K. Matsui, S. Michimasa, T. Motobayashi, D. Nishimura, T. Otsuka, H. Sakurai, Y. Shiga, P. A. Söderström, T. Sumikama, H. Suzuki, R. Taniuchi, Y. Utsuno, J. J. Valiente-Dobón, and K. Yoneda, Evidence for a new nuclear 'magic number' from the level structure of ^{54}Ca, Nature **502**, 207 (2013).

[5] S. Michimasa, M. Kobayashi, Y. Kiyokawa, S. Ota, D. S. Ahn, H. Baba, G. P. A. Berg, M. Dozono, N. Fukuda, T. Furuno, E. Ideguchi, N. Inabe, T. Kawabata, S. Kawase, K. Kisamori, K. Kobayashi, T. Kubo, Y. Kubota, C. S. Lee, M. Matsushita, H. Miya, A. Mizukami, H. Nagakura, D. Nishimura, H. Oikawa, H. Sakai, Y. Shimizu, A. Stolz, H. Suzuki, M. Takaki, H. Takeda, S. Takeuchi, H. Tokieda, T. Uesaka, K. Yako, Y. Yamaguchi, Y. Yanagisawa, R. Yokoyama, K. Yoshida, and S. Shimoura, Magic nature of neutrons in ^{54}Ca: First mass measurements of $^{55-57}$Ca, Phys. Rev. Lett. **121**, 022506 (2018).

[6] L. Lalanne, O. Sorlin, A. Poves, M. Assié, F. Hammache, S. Koyama, D. Suzuki, F. Flavigny, V. Girard-Alcindor, A. Lemasson, A. Matta, T. Roger, D. Beaumel, Y. Blumenfeld, B. A. Brown, F. D. O. Santos, F. Delaunay, N. de Séréville, S. Franchoo, J. Gibelin, J. Guillot, O. Kamalou, N. Kitamura, V. Lapoux, B. Mauss, P. Morfouace, J. Pancin, T. Y. Saito, C. Stodel, and J.-C. Thomas, $N = 16$ Magicity Revealed at the Proton Drip Line through the Study of ^{35}Ca, Phys. Rev. Lett. **131**, 092501 (2023).

[7] A. J. Miller, K. Minamisono, A. Klose, D. Garand, C. Kujawa, J. D. Lantis, Y. Liu, B. Maaß, P. F. Mantica, W. Nazarewicz, W. Nörtershäuser, S. V. Pineda, P. G. Reinhard, D. M. Rossi, F. Sommer, C. Sumithrarachchi, A. Teigelhöfer, and J. Watkins, Proton superfluidity and charge radii in proton-rich calcium isotopes, Nat. Phys. **15**, 432 (2019).

[8] E. Caurier, G. Martínez-Pinedo, F. Nowacki, A. Poves, and A. P. Zuker, The shell model as a unified view of nuclear structure, Rev. Mod. Phys. **77**, 427 (2005).

[9] J. J. Valiente-Dobón, A. Poves, A. Gadea, and B. Fernández-Domínguez, Broken mirror symmetry in ^{36}S and ^{36}Ca, Phys. Rev. C **98**, 011302 (2018).

[10] L. Lalanne, O. Sorlin, A. Poves, M. Assié, F. Hammache, S. Koyama, D. Suzuki, F. Flavigny, V. Girard-Alcindor, A. Lemasson, A. Matta, T. Roger, D. Beaumel, Y. Blumenfeld, B. A. Brown, F. D. O. Santos, F. Delaunay, N. de Séréville, S. Franchoo, J. Gibelin, J. Guillot, O. Kamalou, N. Kitamura, V. Lapoux, B. Mauss, P. Morfouace, M. Niikura, J. Pancin, T. Y. Saito, C. Stodel, and J.-C. Thomas, Structure of ^{36}Ca under the Coulomb Magnifying Glass, Phys. Rev. Lett. **129**, 122501 (2022).

[11] E. Caurier, K. Langanke, G. Martínez-Pinedo, F. Nowacki, and P. Vogel, Shell model description of isotope shifts in calcium, Phys. Lett. B **522**, 240 (2001).

[12] N. Dronchi, D. Weisshaar, B. A. Brown, A. Gade, R. J. Charity, L. G. Sobotka, K. W. Brown, W. Reviol, D. Bazin, P. J. Farris, A. M. Hill, J. Li, B. Longfellow, D. Rhodes, S. N. Paneru, S. A. Gillespie, A. Anthony, E. Rubino, and S. Biswas, Measurement of the $B(E2\uparrow)$ strengths of ^{36}Ca and ^{38}Ca, Phys. Rev. C **107**, 034306 (2023).

[13] B. A. Brown and W. A. Richter, New "USD" Hamiltonians for the *sd* shell, Phys. Rev. C **74**, 034315 (2006).

[14] E. Caurier, F. Nowacki, and A. Poves, Merging of the islands of inversion at $N = 20$ and $N = 28$, Phys. Rev. C **90**, 014302 (2014).

[15] J. A. Tostevin, G. Podolyák, B. A. Brown, and P. G. Hansen, Correlated two-nucleon stripping reactions, Phys. Rev. C **70**, 064602 (2004).

[16] J. A. Tostevin and B. A. Brown, Diffraction dissociation contributions to two-nucleon knockout reactions and the suppression of shell-model strength, Phys. Rev. C **74**, 064604 (2006).

[17] A. Gade and B. M. Sherrill, NSCL and FRIB at Michigan State University: Nuclear science at the limits of stability, Phys. Scr. **91**, 053003 (2016).

[18] D. J. Morrissey, B. M. Sherrill, M. Steiner, A. Stolz, and I. Wiedenhoever, Commissioning the A1900 projectile fragment separator, Nucl. Instrum. Methods Phys. Res. B **204**, 90 (2003).

[19] D. Bazin, J. Caggiano, B. Sherrill, J. Yurkon, and A. Zeller, The S800 spectrograph, Nucl. Instrum. Methods Phys. Res. B **204**, 629 (2003).

[20] J. Yurkon, D. Bazin, W. Benenson, D. J. Morrissey, B. M. Sherrill, D. Swan, and R. Swanson, Focal plane detector for the S800 high-resolution spectrometer, Nucl. Instrum. Methods Phys. Res. A **422**, 291 (1999).

[21] A. Gade, D. Weisshaar, B. Brown, J. Tostevin, D. Bazin, K. Brown, R. Charity, P. Farris, A. Hill, J. Li, B. Longfel-

low, W. Reviol, and D. Rhodes, In-beam γ-ray spectroscopy at the proton dripline: ^{40}Sc, Phys. Lett. B **808**, 135637 (2020).

[22] A. Gade, B. A. Brown, D. Weisshaar, D. Bazin, K. W. Brown, R. J. Charity, P. Farris, A. M. Hill, J. Li, B. Longfellow, D. Rhodes, W. Reviol, and J. A. Tostevin, Dissipative reactions with intermediate-energy beams: A novel approach to populate complex-structure states in rare isotopes, Phys. Rev. Lett. **129**, 242501 (2022).

[23] A. Gade, D. Weisshaar, B. A. Brown, D. Bazin, K. W. Brown, R. J. Charity, P. Farris, A. M. Hill, J. Li, B. Longfellow, D. Rhodes, W. Reviol, and J. A. Tostevin, Exploiting dissipative reactions to perform in-beam γ-ray spectroscopy of the neutron-deficient isotopes ^{38,39}Ca, Phys. Rev. C **106**, 064303 (2022).

[24] S. Paschalis, I. Lee, A. Macchiavelli, C. Campbell, M. Cromaz, S. Gros, J. Pavan, J. Qian, R. Clark, H. Crawford, D. Doering, P. Fallon, C. Lionberger, T. Loew, M. Petri, T. Stezelberger, S. Zimmermann, D. Radford, K. Lagergren, D. Weisshaar, R. Winkler, T. Glasmacher, J. Anderson, and C. Beausang, The performance of the Gamma-Ray Energy Tracking In-beam Nuclear Array GRETINA, Nucl. Instrum. Methods Phys. Res. A **709**, 44 (2013).

[25] D. Weisshaar, D. Bazin, P. C. Bender, C. M. Campbell, F. Recchia, V. Bader, T. Baugher, J. Belarge, M. P. Carpenter, H. L. Crawford, M. Cromaz, B. Elman, P. Fallon, A. Forney, A. Gade, J. Harker, N. Kobayashi, C. Langer, T. Lauritsen, I. Y. Lee, A. Lemasson, B. Longfellow, E. Lunderberg, A. O. Macchiavelli, K. Miki, S. Momiyama, S. Noji, D. C. Radford, M. Scott, J. Sethi, S. R. Stroberg, C. Sullivan, R. Titus, A. Wiens, S. Williams, K. Wimmer, and S. Zhu, The performance of the γ-ray tracking array GRETINA for γ-ray spectroscopy with fast beams of rare isotopes, Nucl. Instrum. Methods Phys. Res. A **847**, 187 (2017).

[26] M. Wang, G. Audi, A. H. Wapstra, F. G. Kondev, M. MacCormick, X. Xu, and B. Pfeiffer, The Ame2012 atomic mass evaluation, Chin. Phys. C **36**, 1603 (2012).

[27] P. Doornenbal, P. Reiter, H. Grawe, T. Otsuka, A. Al-Khatib, A. Banu, T. Beck, F. Becker, P. Bednarczyk, G. Benzoni, A. Bracco, A. Bürger, L. Caceres, F. Camera, S. Chmel, F. Crespi, H. Geissel, J. Gerl, M. Górska, J. Grębosz, H. Hübel, M. Kavatsyuk, O. Kavatsyuk, M. Kmiecik, I. Kojouharov, N. Kurz, R. Lozeva, A. Maj, S. Mandal, W. Meczynski, B. Million, Z. Podolyák, A. Richard, N. Saito, T. Saito, H. Schaffner, M. Seidlitz, T. Striepling, Y. Utsuno, J. Walker, N. Warr, H. Weick, O. Wieland, M. Winkler, and H. Wollersheim, The $T = 2$ mirrors ^{36}Ca and ^{36}S: A test for isospin symmetry of shell gaps at the driplines, Phys. Lett. B **647**, 237 (2007).

[28] A. Bürger, F. Azaiez, A. Algora, A. Al-Khatib, B. Bastin, G. Benzoni, R. Borcea, C. Bourgeois, P. Bringel, E. Clément, J.-C. Dalouzy, Z. Dlouhý, Z. Dombrádi, A. Drouart, C. Engelhardt, S. Franchoo, Z. Fülöp, A. Görgen, S. Grévy, H. Hübel, F. Ibrahim, W. Korten, J. Mrázek, A. Navin, F. Rotaru, P. Roussel Chomaz, M.-G. Saint-Laurent, G. Sletten, D. Sohler, O. Sorlin, M. Stanoiu, I. Stefan, C. Theisen, C. Timis, D. Verney, and S. Williams, Cross sections for one-neutron knockout from ^{37}Ca at intermediate energy, Phys. Rev. C **86**, 064609 (2012).

[29] S. Agostinelli, J. Allison, K. Amako, J. Apostolakis, H. Araujo, P. Arce, M. Asai, D. Axen, S. Banerjee, G. Barrand, F. Behner, L. Bellagamba, J. Boudreau, L. Broglia, A. Brunengo, H. Burkhardt, S. Chauvie, J. Chuma, R. Chytracek, G. Cooperman, G. Cosmo, P. Degtyarenko, A. Dell'Acqua, G. Depaola, D. Dietrich, R. Enami, A. Feliciello, C. Ferguson, H. Fesefeldt, G. Folger, F. Foppiano, A. Forti, S. Garelli, S. Giani, R. Giannitrapani, D. Gibin, J. G. Cadenas, I. González, G. G. Abril, G. Greeniaus, W. Greiner, V. Grichine, A. Grossheim, S. Guatelli, P. Gumplinger, R. Hamatsu, K. Hashimoto, H. Hasui, A. Heikkinen, A. Howard, V. Ivanchenko, A. Johnson, F. Jones, J. Kallenbach, N. Kanaya, M. Kawabata, Y. Kawabata, M. Kawaguti, S. Kelner, P. Kent, A. Kimura, T. Kodama, R. Kokoulin, M. Kossov, H. Kurashige, E. Lamanna, T. Lampén, V. Lara, V. Lefebure, F. Lei, M. Liendl, W. Lockman, F. Longo, S. Magni, M. Maire, E. Medernach, K. Minamimoto, P. M. de Freitas, Y. Morita, K. Murakami, M. Nagamatu, R. Nartallo, P. Nieminen, T. Nishimura, K. Ohtsubo, M. Okamura, S. O'Neale, Y. Oohata, K. Paech, J. Perl, A. Pfeiffer, M. Pia, F. Ranjard, A. Rybin, S. Sadilov, E. D. Salvo, G. Santin, T. Sasaki, N. Savvas, Y. Sawada, S. Scherer, S. Sei, V. Sirotenko, D. Smith, N. Starkov, H. Stoecker, J. Sulkimo, M. Takahata, S. Tanaka, E. Tcherniaev, E. S. Tehrani, M. Tropeano, P. Truscott, H. Uno, L. Urban, P. Urban, M. Verderi, A. Walkden, W. Wander, H. Weber, J. Wellisch, T. Wenaus, D. Williams, D. Wright, T. Yamada, H. Yoshida, and D. Zschiesche, GEANT4 – a simulation toolkit, Nucl. Instrum. Methods Phys. Res. A **506**, 250 (2003).

[30] J. Allison, K. Amako, J. Apostolakis, P. Arce, M. Asai, T. Aso, E. Bagli, A. Bagulya, S. Banerjee, G. Barrand, B. Beck, A. Bogdanov, D. Brandt, J. Brown, H. Burkhardt, P. Canal, D. Cano-Ott, S. Chauvie, K. Cho, G. Cirrone, G. Cooperman, M. Cortés-Giraldo, G. Cosmo, G. Cuttone, G. Depaola, L. Desorgher, X. Dong, A. Dotti, V. Elvira, G. Folger, Z. Francis, A. Galoyan, L. Garnier, M. Gayer, K. Genser, V. Grichine, S. Guatelli, P. Guèye, P. Gumplinger, A. Howard, I. Hřivnáčová, S. Hwang, S. Incerti, A. Ivanchenko, V. Ivanchenko, F. Jones, S. Jun, P. Kaitaniemi, N. Karakatsanis, M. Karamitros, M. Kelsey, A. Kimura, T. Koi, H. Kurashige, A. Lechner, S. Lee, F. Longo, M. Maire, D. Mancusi, A. Mantero, E. Mendoza, B. Morgan, K. Murakami, T. Nikitina, L. Pandola, P. Paprocki, J. Perl, I. Petrović, M. Pia, W. Pokorski, J. Quesada, M. Raine, M. Reis, A. Ribon, A. R. Fira, F. Romano, G. Russo, G. Santin, T. Sasaki, D. Sawkey, J. Shin, I. Strakovsky, A. Taborda, S. Tanaka, B. Tomé, T. Toshito, H. Tran, P. Truscott, L. Urban, V. Uzhinsky, J. Verbeke, M. Verderi, B. Wendt, H. Wenzel, D. Wright, D. Wright, T. Yamashita, J. Yarba, and H. Yoshida, Recent developments in GEANT4, Nucl. Instrum. Methods Phys. Res. A **835**, 186 (2016).

[31] L. Riley, D. Weisshaar, H. Crawford, M. Agiorgousis, C. Campbell, M. Cromaz, P. Fallon, A. Gade, S. Gregory, E. Haldeman, L. Jarvis, E. Lawson-John, B. Roberts, B. Sadler, and C. Stine, UCGretina GEANT4 simulation of the GRETINA Gamma-Ray Energy Tracking Array, Nucl. Instrum. Methods Phys. Res. A **1003**, 165305 (2021).

[32] D. Bazin, B. A. Brown, C. M. Campbell, J. A. Church, D. C. Dinca, J. Enders, A. Gade, T. Glasmacher, P. G.

Hansen, W. F. Mueller, H. Olliver, B. C. Perry, B. M. Sherrill, J. R. Terry, and J. A. Tostevin, New Direct Reaction: Two-Proton Knockout from Neutron-Rich Nuclei, Phys. Rev. Lett. **91**, 012501 (2003).

[33] K. Yoneda, A. Obertelli, A. Gade, D. Bazin, B. A. Brown, C. M. Campbell, J. M. Cook, P. D. Cottle, A. D. Davies, D.-C. Dinca, T. Glasmacher, P. G. Hansen, T. Hoagland, K. W. Kemper, J.-L. Lecouey, W. F. Mueller, R. R. Reynolds, B. T. Roeder, J. R. Terry, J. A. Tostevin, and H. Zwahlen, Two-neutron knockout from neutron-deficient ^{34}Ar, ^{30}S, and ^{26}Si, Phys. Rev. C **74**, 021303 (2006).

[34] E. C. Simpson, J. A. Tostevin, D. Bazin, B. A. Brown, and A. Gade, Two-Nucleon Knockout Spectroscopy at the Limits of Nuclear Stability, Phys. Rev. Lett. **102**, 132502 (2009).

[35] E. C. Simpson, J. A. Tostevin, D. Bazin, and A. Gade, Longitudinal momentum distributions of the reaction residues following fast two-nucleon knockout reactions, Phys. Rev. C **79**, 064621 (2009).

[36] E. C. Simpson and J. A. Tostevin, Correlations probed in direct two-nucleon removal reactions, Phys. Rev. C **82**, 044616 (2010).

[37] B. Longfellow, A. Gade, J. A. Tostevin, E. C. Simpson, B. A. Brown, A. Magilligan, D. Bazin, P. C. Bender, M. Bowry, B. Elman, E. Lunderberg, D. Rhodes, M. Spieker, D. Weisshaar, and S. J. Williams, Two-neutron knockout as a probe of the composition of states in ^{22}Mg,^{23} Al, and ^{24}Si, Phys. Rev. C **101**, 031303 (2020).

[38] S. R. Stroberg, A. Gade, J. A. Tostevin, V. M. Bader, T. Baugher, D. Bazin, J. S. Berryman, B. A. Brown, C. M. Campbell, K. W. Kemper, C. Langer, E. Lunderberg, A. Lemasson, S. Noji, F. Recchia, C. Walz, D. Weisshaar, and S. J. Williams, Single-particle structure of silicon isotopes approaching ^{42}Si, Phys. Rev. C **90**, 034301 (2014).

[39] A. Magilligan and B. A. Brown, New isospin-breaking "USD" Hamiltonians for the *sd* shell, Phys. Rev. C **101**, 064312 (2020).

[40] For $\log_{10}(T9) < 0.3$, the $^{35}\mathrm{K}(p,\gamma)^{36}\mathrm{Ca}$ rate is dominated by the 2_1^+ state for which all of the needed properties have been measured and are given in Tab. VI of Ref. [12]. At higher temperatures the 1_1^+ and 2_2^+ states, which partially rely on shell-model calculations, start to contribute. Here, standard ZBM2 deviates less than 10% from the ZBM2gap results.